Crowdsourced air temperature data for the evaluation of urban microscale simulations: Insights into spatiotemporal patterns from three German cities

Lara van der Linden[1*], Björn Maronga[2☯] and Benjamin Bechtel[1☯]

1 Bochum Urban Climate Lab, Institute of Geography, Ruhr-University Bochum, Bochum, Germany
2 Leibniz University Hannover, Institute of Meteorology and Climatology, Hannover, Germany

☯These authors contributed equally to this work.
* lara.vanderlinden@rub.de

Abstract

Rapid development of microscale urban climate models in recent years requires ongoing model evaluation under different scenarios and conditions. In a previous study, we utilised crowdsourced air temperature data from Netatmo citizen weather stations (CWS) for the evaluation of the PALM model during a hot summer day in the city of Bochum, Germany. The data proved valuable due to their high spatial resolution, even though a temporal pattern in model performance with an underestimation of air temperatures at night was observed. However, this finding was based on a single city and limited episode.

In this paper, PALM simulations for three cities with different size and geographical setting in Germany (Dortmund, Cologne, and Berlin) are compared with respective crowdsourcing data to test the potential and robustness of this approach. Each simulation covers a period of three days during an observed heat wave in August 2020.

The model evaluation with crowdsourced data reveals a high model performance in all cities. At the same time, temporal and spatial patterns in the differences between the modelled and crowdsourced data can be detected, confirming the underestimation of nighttime air temperature by the model especially in densely built areas, as was found in the precursor study. Nevertheless, the simulations show that the PALM model is capable of compensating a great share of the differences between mesoscale model predictions and observed temperatures. Overall, we find that crowdsourced data is an easily available tool for model evaluation and that the PALM model shows a high accuracy over a range of different cities and geographical settings.

Introduction

Urban areas play a central role in providing living space, work, and recreation with more than half of the worlds population living in urban areas [1]. At the same time, they are especially vulnerable to heat as a result of the strong modification of the natural environment. The occurrence of sealed surfaces and the presence of buildings modifies the thermal and aerodynamic conditions within the city, leading to higher air temperatures, especially at night, known as the urban heat island (UHI). The UHI varies spatially and temporally within the cities, forming local cool and hot spots depending on the density of the urban structure and the presence of sealed and natural surfaces [2].

Summer heat in urban areas can lead to diverse negative effects. Heat causes a reduction of productivity and therefore, economical losses in Europe [3, 4] and even higher econonomical costs globally [5]. Furthermore, heat can cause negative health effects such as heat strokes leading to a higher mortality. Vulnerable population groups include children, elderly people and adults with chronic diseases [6]. This problem is further intensified in combination with air pollution. The hot summer of 2022 in Europe is estimated to have caused more than 60.000 heat-related deaths in 35 European countries [7] while the European heatwave of 2003 caused more than 70.000 additional deaths [8]. Heaviside et al. [9] attributed 50 % of the heat-related deaths of 2003 in the Midlands in the UK to the UHI revealing that the UHI further exacerbates the health risks associated with heat. The ongoing climate change has already increased the frequency and intensity of heatwaves globally. Projected climate change for different global warming levels is expected to further increment the occurrence and intensity of heatwaves. Even with a global warming level of 1.5 °C a 10 year heat event is four times more likely to occur compared to a pre-industrial climate [10].

This combination of the urban heat island, heat waves and climate change creates a need for climate adaptation in cities to counteract the negative effects of overheated urban areas [11, 12]. To efficiently plan, evaluate and implement adaptation measures, detailed information on the urban microclimate is required. The most common tool to generate this information are numerical models [13, 14]. Microscale models like ENVI-met [15], uDALES [16], or PALM [17] resolve the three-dimensional urban structure and deliver urban microclimatic conditions with a high resolution of a few metres or less. Aside from modelling the current microclimatic conditions, these models enable comparative studies to asses the efficiency of different adaptation strategies [18–20]. The PALM model system is capable of resolving microscale processes, including turbulent transport, while considering mesoscale weather influences through nesting [17]. The dynamic core of the model was successfully evaluated against wind-tunnel experiment [21]. Furthermore, extensive measurement campaigns in Prague verified the models performance with respect to surface interactions in a real urban environment [22]. Nevertheless, the evaluation is limited to these specific case studies and further validation with measurement data with a high spatial coverage is currently missing.

As model performance can vary between different environments and meteorological conditions, simulations should be evaluated for comparable conditions to ensure reliable results. Professional weather stations usually do not provide the spatial resolution required for model evaluation on the microscale [23]. Measurement campaigns deliver high-quality and targeted evaluation data. The disadvantages of measurement campaigns are, however, their high costs and limited temporal and spatial coverage [24, 25]. Thus, observational data for a specific area of study are often the bottleneck for model performance evaluation. Crowdsourced meteorological data can potentially bridge this gap and have been successfully applied for this purpose in first case studies [26, 27]. The number of citizen weather stations (CWS) is constantly increasing and data are often made available through application programming interfaces (APIs) [24]. A popular source of crowdsourced air temperature data are the CWS produced by the company Netatmo. Different quality control procedures have been developed and improved in recent years to ensure a high data quality to use the data for research purposes [28–30]. The quality controlled data have been applied to study the canopy urban heat island on a local scale [31], combined with remote sensing data and machine learning to spatially model the air temperature in Berlin [25] and most recently applied to detect urban heat advection [32].

In a precursor study [26], we used crowdsourced air temperature data from Netatmo stations in the Bochum (Germany) area to evaluate results of the PALM model for a

summer day. The evaluation showed a good agreement between the model and measurements, but also revealed an underestimation of nighttime air temperatures in PALM. Žuvela-Aloise et al. [27] applied crowdsourced air temperature data for model evaluation in Vienna for a city-wide simulation without resolving the three-dimensional structure of the city. Their results reveal a good model performance when comparing the model results with crowdsourced data and professional measurements. At the same time, they detected spatial and temporal patterns in the differences between the modelled and measured data.

While both studies demonstrated the considerable potential for using crowdsourced data for model evaluation, they are specific case studies for one city each with and without explicitly resolving the three-dimensional structure of the city. To further explore this approach, we simulated a summer period in three German cities and evaluated the results with crowdsourced air temperature data to answer the following research questions:

- To what extent does the microscale large eddy simulation (LES) model PALM improve the representation of the urban thermal effect in relation to the mesoscale forcing data?
- Are there any temporal and / or spatial patterns in the differences between the modelled and crowdsourced data and what causes these spatiotemporal patterns? Can differences be attributed to errors in either the model or the crowdsourced data?
- What are the benefits and limitations of model evaluation with crowdsourced air temperature data? Is the model evaluation with crowdsourced data consistent between different cities?

Materials and methods

Study period and areas

The study areas are located in three German cities: Dortmund, Cologne, and Berlin. The cities were chosen based on their characteristics and the availability of open geospatial datasets. Dortmund is located in western Germany in the Ruhr area, a metropolitan area consisting of many neighbouring cities. Dortmund is the smallest of the three cities with 598.246 inhabitants and a size of 280.71 km^2. Cologne is located south-west of Dortmund on the Rhine river, with 1.017.355 inhabitants and a size of 405.01 km^2. Germany's capital Berlin lies in eastern Germany and is more isolated from other urbanised environments than either Dortmund and Cologne. At the same time, it is the largest city with 3.596.999 inhabitants and a size of 891.12 km^2 [33].

The study period covers a 72 hour period from 6th to 9th August 2020 06:00 h UTC within a week long heatwave. The weather was dominated by high pressure systems with low wind speeds, high solar radiation, and high daytime air temperatures. The meteorological conditions for the three cities are listed in Table 1. As there is no station from the German Weather Service (DWD) in Dortmund, the data from the closest station in Essen is displayed.

PALM model configuration

Model description and configuration

The PALM model system version 23.10 was applied for Dortmund and Cologne and version 24.04 for Berlin. The change in versions for Berlin was necessary due to a change

Table 1. Meteorological conditions for the three studied cities

City	Dortmund	Cologne	Berlin
Weather type	anticyclonic	anticyclonic	anticyclonic
Minimum air temperature	20.2 °C	15.1 °C	16.0 °C
Maximum air temperature	34.3 °C	36.8 °C	35.5 °C
Minimum relative humidity	23.0 %	19.0 %	21.0 %
Maximum relative humidity	70.0 %	76.0 %	82.0 %
Cloudiness	mostly clear sky, scattered high clouds on 6th August, cloud cover on 9th August	mostly clear sky, scattered high clouds on 6th August, cloud cover on 9th August	occasional scattered high or low clouds
Mean wind speed	2.24 m s^{-1}	2.37 m s^{-1}	2.17 m s^{-1}

Weather type classification derived from the Objective Weather Type Classification Data of the DWD [34, 35], meteorological statistics derived from observational data from the measurement network of the DWD [36–39]

in the operating system on the HPC cluster where the simulations were conducted. The PALM model solves the incompressible Navier-Stokes equations with the Boussinesq approximation. Turbulence closure follows the 1.5-order Deardoff's [40] approach with the refinements of Moeng and Wyngaard [41] and Saiki et al. [42]. The 5th order upwind advection scheme by Wicker and Skamarok [43] as well as the 3rd order Runge-Kutta timestep scheme [44] were applied. Pressure was solved with the multigrid-scheme of the Poisson equation. Boundary conditions at the surface are modelled according to the Monin-Obukhov similarity theory. The following modules were applied in this study: land surface model (LSM) [45], building surface model (BSM) [46], plant canopy model (PCM) and radiative transfer model (RTM) [47], radiation model [17], biometeorology model (BIO) [48], offline nesting [49] and online nesting [50]. Within the radiation model, the RRTMG model was used to provide background fluxes for shortwave and longwave radiation. A detailed model description can be found in Maronga et al. [17].

For each city, three modelling domains were defined to incorporate regional weather influences through offline nesting and modelling microscale processes in the urban canyon. Domain layouts with the number of grid cells in x, y and z direction (nx, ny, nz) and the horizontal and vertical grid spacing (dx, dy, dz) are described in Table 2. The simulations were conducted for 72 hours in Dortmund and Berlin and for 66 hours in Cologne. At the start of the simulations, PALMs spinup mechanism [17] was applied for 24 hours to initialise soil temperature and water content as well as wall/roof material temperatures without turning on the atmospheric code to save computational time and realise realistic initial conditions.

Static input data

PALM requires detailed information on the urban surface, which can be provided by means of a so-called static driver [51]. Due to the horizontal resolution of 32 m in the parent domains, the three-dimensional urban structure was not explicitly resolved. The static drivers for the parent domains contain the land surface descriptions (pavement, vegetation and water types) derived from the CORINE Land Cover 2018 dataset [52], soil types [53, 54] and topographic information [55]. To account for an urban effect, the roughness length *z0* for pavement types 1, 2 and 3 were modified within the static driver and set to 2.0 for pavement type 1 and 1.5 for pavement types 2 and 3.

For the child domains with a higher resolution the three-dimensional structure was explicitly resolved. Information on land surface description (pavement, vegetation and water types) was derived from ALKIS cadastral data [56, 57] and further refined with the Copernicus Imperviousness dataset [58] as, e.g., gardens are not defined separately within the cadastral data. The building geometries were included in the LoD2 CityGML

Table 2. Domain layouts and grid resolutions for all three cities

Domain	nx	ny	nz	dx/dy	dz
Dortmund					
Parent	864	864	200	32 m	16 m
Child 1	1120	1104	240	8 m	4 m
Child 2	992	1008	200	2 m	2 m
Cologne					
Parent	896	864	200	32 m	16 m
Child 1	992	1008	240	8 m	4 m
Child 2	992	1008	200	2 m	2 m
Berlin					
Parent	960	936	180	32 m	16 m
Child 1	992	1008	200	8 m	4 m
Child 2	992	1008	200	2 m	2 m

datasets from the federal states of North-Rhine Westphalia and Berlin [59, 60], whereas building age was extracted from the gridded zensus data [61, 62] and combined with the building geometries. Each building was then classified into PALM building types, depending on age information. However, age information only exists for residential buildings. All non-residential buildings were assigned to building type 5 which describes non-residential buildings built between 1950 and 2000. Topography information was provided by high resolution digital elevation models from the federal states [63, 64]. The positions and heights of trees were extracted from airborne LiDAR datasets [65, 66] and processed into a canopy height model from the difference between the digital elevation models and the digital surface models [67, 68].

The datasets were processed to GeoTIFF files in the corresponding resolution for each domain and city. Using the GEO4PALM tool [69], the GeoTIFF files were then processed according to the PALM Input Data Standard (PIDS) in the static driver for each domain. All data sources are listed in S1 Table.

The resulting surface descriptions, building, and tree positions for the two child domains of the three cities are presented in Fig 1. The child domains in Berlin cover dense urban structures with a few larger green spaces such as the Tiergarten and Tempelhofer Feld. Furthermore, the Spree river flows from the south-east to the north-west through the domain. In Cologne, the dense city centre is surrounded by a green belt. Outside the green belt, the urban structure is less dense and interspersed with green areas. The large Rhine river flows from the south to the north through the city. Dortmund is the smallest city, and the child domains therefore cover more areas with a lower density of buildings and sealed areas. The densely built city centre is covered by the child domains, as well as larger sealed areas in the harbour north of the city centre.

Initial and boundary conditions

The initial and boundary conditions were derived from the COSMO-D2 analysis data [71]. COSMO-D2 is the former regional weather model of the DWD. The *inifor* preprocessor tool included in PALM was used to generate the required meteorological boundary conditions from the analysis data. *Inifor* transforms and interpolates the potential temperature, specific humidity, and the velocity components from the COSMO grid to the PALM model grid [49].

In addition, the initial soil temperature and soil moisture were extracted from the COSMO-D2 dataset. In Berlin, the initial soil moisture exceeded the saturation

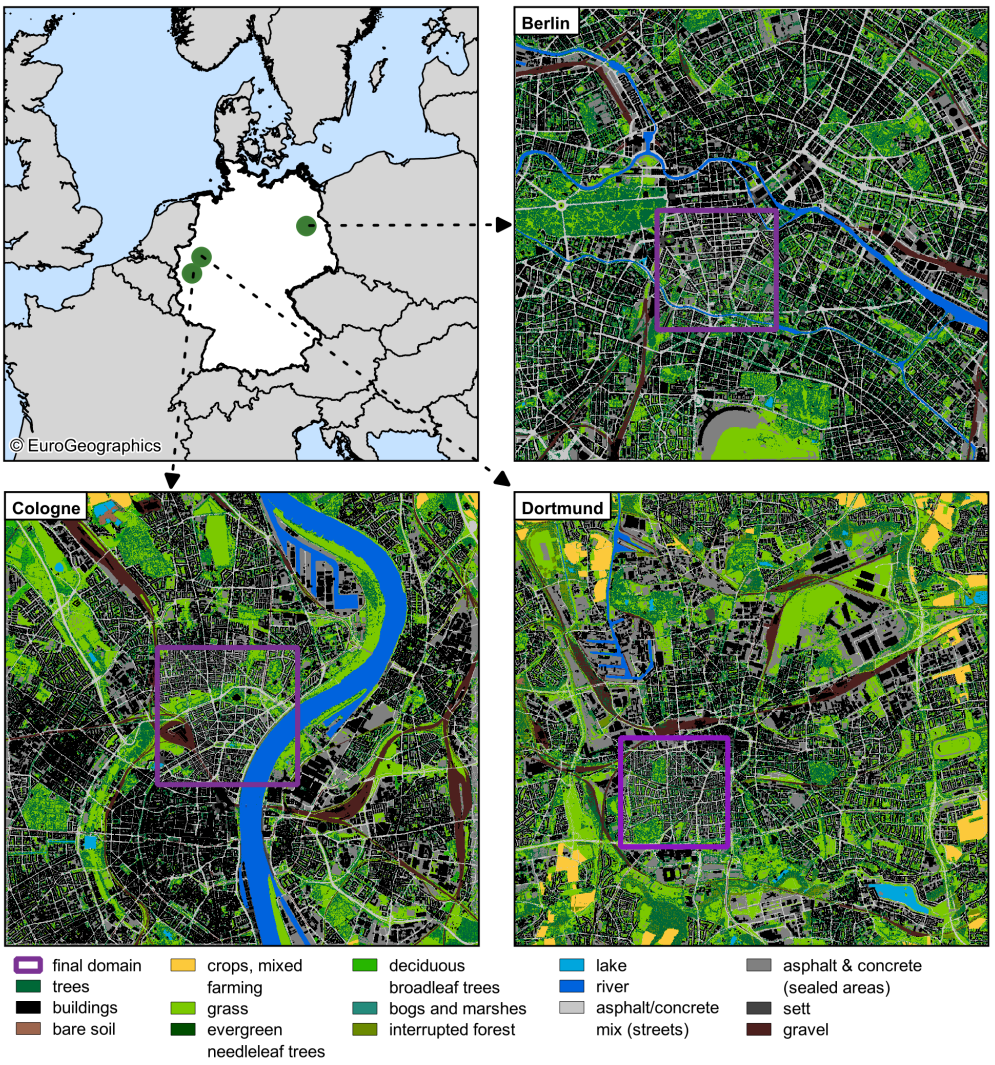

Fig 1. Location of the studied cities within Germany (top left) and land surface description, building and tree position for the child domains of Berlin (top right), Cologne (bottom left) and Dortmund (bottom right). European country outlines are derived from the NUTS dataset of the European Commission [70]

moisture of the coarse soil types assigned within the static driver. As this can lead to numerical instabilities within the model and considering dry conditions in summer 2020, the initial soil moisture was adjusted to the monthly value of field capacity (30 %) for August 2020 [72].

PALM output processing

For model evaluation, the 2 m air temperature is extracted from the averaged $x-y$-cross-section datasets generated by PALM and saved as georeferenced GeoTIFF files for each simulation hour. Before joining the PALM air temperature data with the crowdsourced air temperature, the values at the location of buildings are clipped, as this is the air temperature above the roof. For every station, the results of the PALM model of the station grid cell as well as the surrounding 24 grid cells are extracted and

averaged (averaging radius 2).

Evaluation dataset

The crowdsourced air temperature data was regularly collected into a database by the Bochum Urban Climate Lab. During the collection process, the quality control procedure by Fenner et al. [30] is applied automatically. A detailed description of the dataset is provided by Kittner et al. [73].

The crowdsourced air temperature data was compared with the modelled air temperature data for each station. If a station had a data availability of less than 80 % in the modelled period, the station was excluded from the evaluation.

Results & Discussion

First, the modelled air temperatures and their spatial pattern will be described. Then the model output (hereafter PALM data) will be evaluated with crowdsourced data (hereafter CROWD data). Spatiotemporal differences will be described and their relation to model inaccuracies discussed. Finally, the characteristics of the CROWD data will be examined.

Model results

Fig 2 shows the PALM 2 m air temperatures and deviations from the domain-averaged values for three selected hours on the second day of the simulations. Temporal and spatial patterns in all three cities are well visible. At midday (12:00 UTC), maximum air temperatures of more than 30 °C are calculated in all three cities. Open spaces exposed to solar irradiation are slightly warmer. Areas close to the water, e.g. near the rivers in Cologne and Berlin or forested areas, e.g. in the south of Dortmund show the lowest air temperatures. The early evening after sunset (22:00 UTC) shows a more distinct spatial pattern. While unsealed and open areas cool down rapidly, sealed and densely built areas remain warmer, resulting in higher air temperatures. Park areas within the urban fabric, like the green belt in Cologne or Tiergarten park in Berlin form local cool islands. In the southern part of Dortmund, local cool islands develop due to topographic effects where the cool area accumulates in valleys. Throughout the night, open areas continue to cool down more rapidly than built areas. Towards the end of the night these areas reach air temperatures below 20 °C, while the denser city areas remain warmer.

The observed temporal and spatial pattern clearly follows the concept of the canopy layer urban heat island [2]. At daytime, spatial differences in air temperature are lower, and exposed areas are the warmest. Once cooling after sunset starts, exposed and especially vegetated areas cool down more rapidly. Built areas exhibit a limited cooling process due to obstructions of the sky and heat release from the urban fabric, especially from sealed surfaces. The PALM model apparently captures such spatially varying air temperatures well, as already reported in previous studies [27, 46].

Model evaluation

To exclude any influence of PALM data averaging, different radii for averaging the PALM data were applied and the evaluation metrics calculated. The first averaging radius (radius one) covers the grid cell of the Netatmo station and the eight surrounding grid cells. For each averaging radius, another set of surrounding grid cells is added each time until a radius of 10 grid cells around the cell containing the station is reached. The recalculated metrics for each radius show only slight differences indicating that the

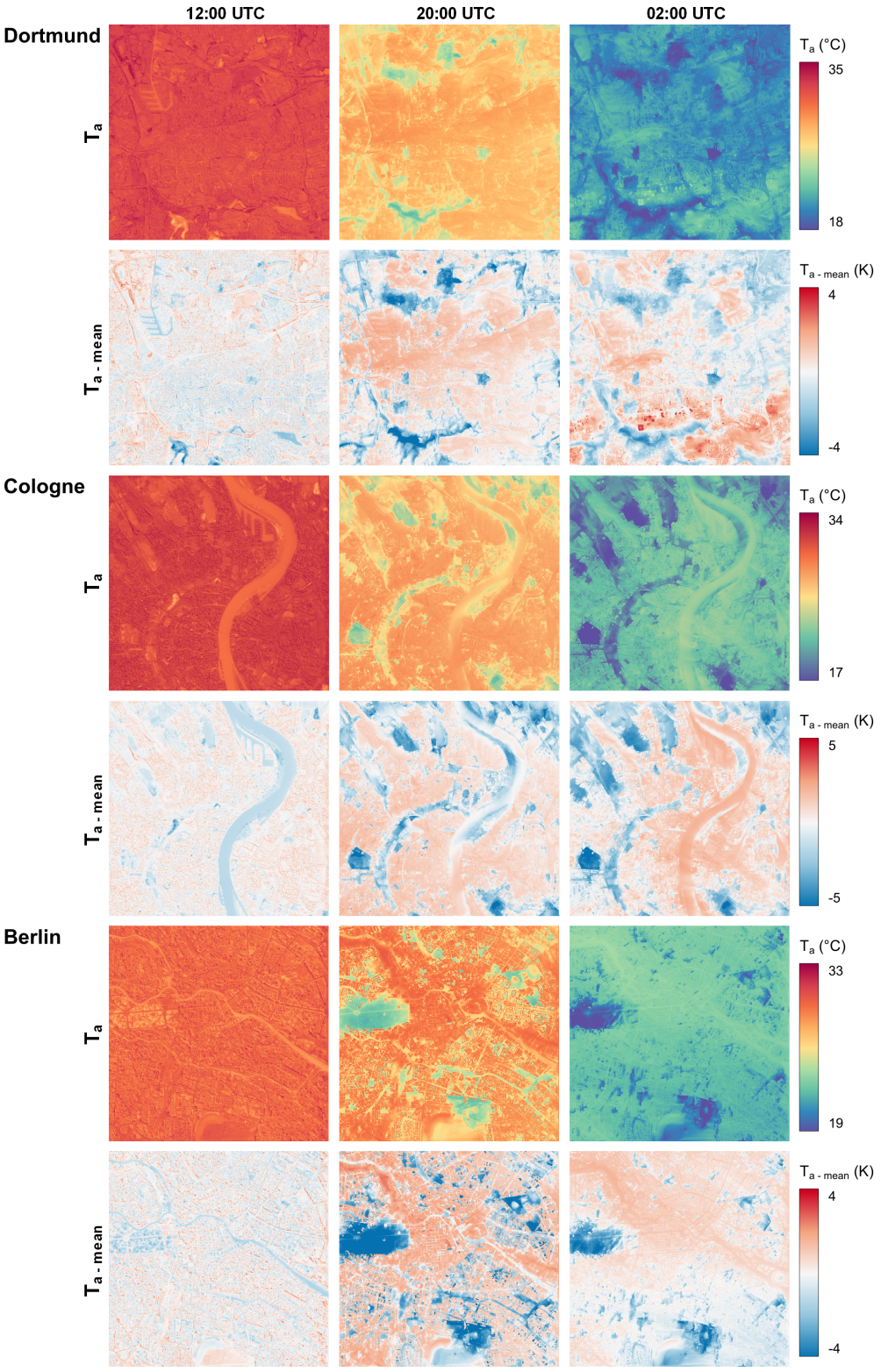

Fig 2. Modelled 2 m air temperature (°C) and air temperature differences (K) for the first child domains in Berlin, Cologne and Dortmund at three selected timesteps. Air temperatures are taken from the second simulated day: 7th of August 2020 12:00 UTC and 20:00 UTC and 8th of August 2020 02:00 UTC. Air temperature differences are calculated from the domain averaged mean air temperature of every hour

averaging radius does not effect the evaluation metrics profoundly. As an averaging radius of one leads to missing data in the second child domains due to the location of these data points only within building grid cells, the averaging radius of two is used for the evaluation.

Comparing the PALM 2 m air temperature to the CROWD air temperature data reveals general good agreement for all three cities, based on the evaluation metrics (Table 3). The mean air temperature and standard deviation for the PALM and CROWD data are closest for Dortmund. For Cologne and Berlin, the PALM mean air temperature is lower than the CROWD mean air temperature. In all three cities, the Pearson correlation coefficient, the determination coefficient R^2, and the index of agreement show a high agreement between the PALM and CROWD data. By the same token, the bias indicates an underestimation of the air temperature by the model in Cologne and Berlin.

The evaluation metrics for the second child domains with a horizontal resolution of 2 m show similar results as for the first child domain in all three cities (see S2 Table). However, due to the smaller domain area, less Netatmo CWS are present for evaluation. Therefore, we focus on the first child domains, since the validity of the evaluation is higher.

Table 3. Evaluation metrics for the first child domain (8 m horizontal resolution) in all three cities

	Dortmund		**Cologne**		**Berlin**	
	PALM	Netatmo	PALM	Netatmo	PALM	Netatmo
Mean (°C)	26.85	27.01	26.98	28.15	26.13	27.12
SD (°C)	4.75	4.79	4.88	4.67	4.28	3.69
Evaluation metrics						
Pearson r	0.93		0.94		0.92	
R^2	0.86		0.88		0.85	
RMSE (°C)	1.83		2.08		1.94	
IoA	0.96		0.95		0.94	
Bias (°C)	0.16		1.17		0.99	
n stations	58		68		116	

Fig 3 presents time series of the PALM and CROWD air temperatures. For comparison the air temperature at the boundaries of the parent domain, provided by the COSMO-D2 mesoscale forcing data (hereafter referred to as COSMO data), is displayed to allow an evaluation how both COSMO and PALM deviate from observations. This shows to which extend PALM can improve the urban signal in comparison to the COSMO forcing. The plots show that the daily cycle of warming and cooling is well captured across the three cities in both models and the observations. This finding is consistent with a previous evaluation study using professional measurement data which demonstrated a good representation of the diurnal cycle by PALM [22]. Notably, the CROWD air temperature range is generally higher than the PALM air temperature range in all cities. This finding aligns with two studies from Vienna that evaluated the model with low-cost sensors [74] and crowdsourced data [27].

In Dortmund both CROWD and PALM data show a stronger daily cycle than the COSMO forcing data with higher daytime air temperatures. The PALM data show a slight underestimation of nighttime air temperatures, especially during the third night.

Similar to the findings for Dortmund, daytime air temperatures in Cologne exceed those of the COSMO forcing data in both the PALM and CROWD data. At night, the measured air temperatures align well with the boundary conditions, whereas PALM tends to underestimate nighttime air temperatures.

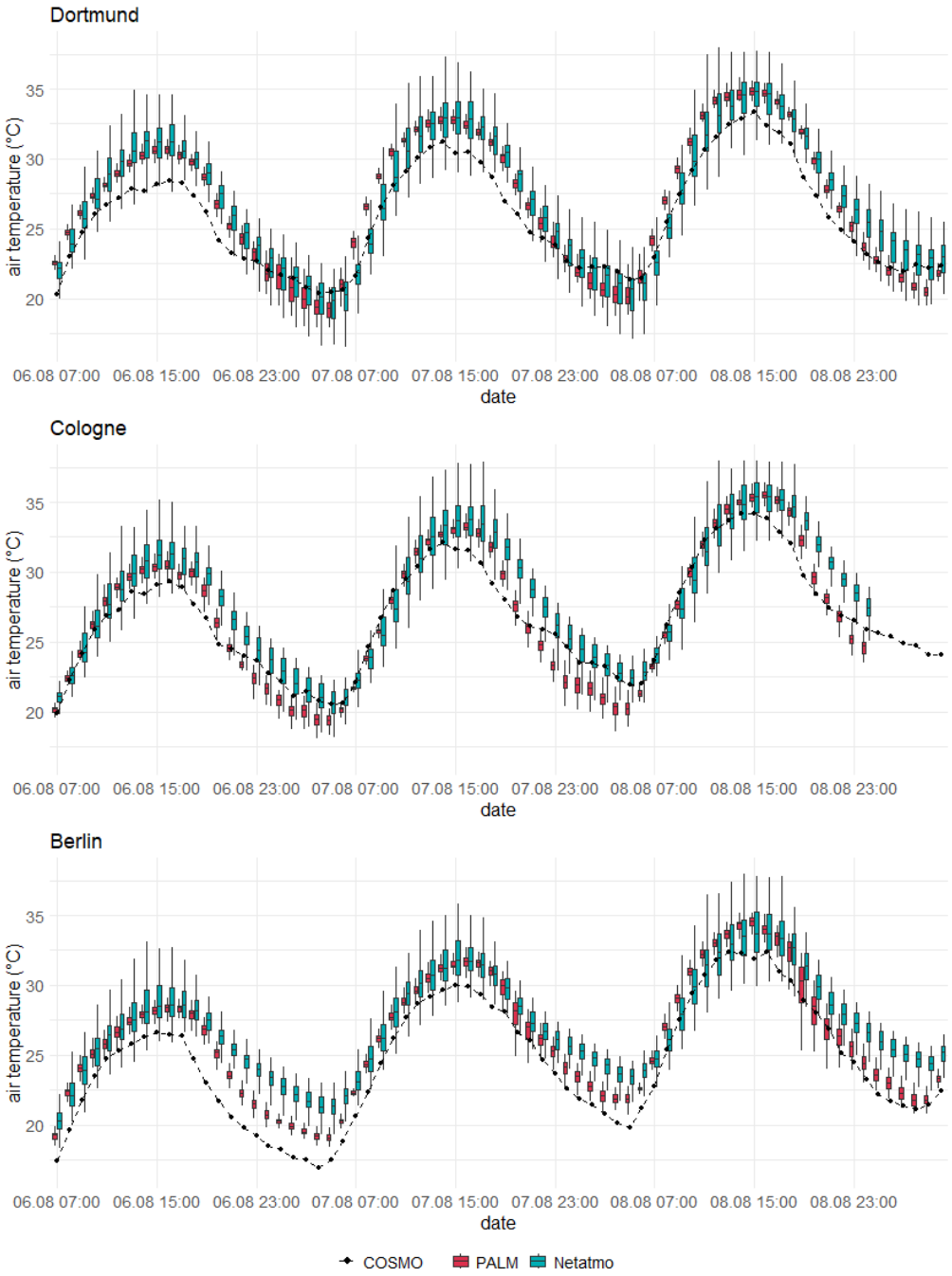

Fig 3. Time series of the modelled and measured air temperature (°C) for the first child domains at the measurement locations as well as the air temperature boundary conditions (°C) from the COSMO model at the boundaries of the parent domains in Berlin, Cologne and Dortmund covering the simulated period from the 6th of August 07:00 UTC to the 9th of August 06:00 UTC. Red box plots represent the modelled air temperature, blue box plots the measured air temperature. The black dots and dashed line are the air temperature boundary conditions from the COSMO model.

Finally, PALM and CROWD data reveal higher daytime and nighttime air temperatures compared to COSMO for the Berlin case. Compared to the measurements, nighttime air temperatures are clearly underestimated by PALM. The COSMO model reveals even lower air temperatures. As a consequence, PALM appears to compensate for much of this cold bias. Overall, this results in the PALM air temperatures exhibiting the strongest diurnal cycle, whereas the CROWD data show a weaker nighttime cooling.

The higher daytime air temperatures in the PALM model compared to the COSMO forcing data are consistent with a previous study for Stuttgart (Germany) by Anders et al. [20]. In comparison to the COSMO forcing data in Berlin, their study also showed low nighttime air temperatures in the COSMO data and PALM's capability to correct low air temperatures. However, in their study, COSMO showed the highest amplitude, while the above results revealed a lower amplitude in the COSMO data in all three cities.

Consistent with previous studies, the diurnal cycle is well represented within PALM. Overall differences between the PALM and CROWD data are small and the evaluation metrics reveal a good model performance. Comparing the diurnal cycles for all three cities, it becomes evident that PALM reliably corrects the cold bias during daytime. In contrast, the nighttime behaviour is less clear and remains ambiguous. This will be analysed in more detail below.

Spatiotemporal patterns in model accuracy

As the plotted time series above reveal diurnally varying model accuracy, temporal clusters were defined covering the warmest hours (14:00–16:00 UTC), the coldest hours (03:00–06:00 UTC), and three-hour periods during warming (08:00–11:00 UTC) and cooling (19:00–22:00 UTC). Evaluation metrics were calculated for each cluster and are presented in Table 4. The Pearson correlation coefficient, coefficient of determination R^2, and index of agreement all indicate better model performance during the warming and cooling periods in Dortmund and Cologne, with the weakest agreement occurring during the coldest hours. This pattern, however, is not evident in the Berlin results. Nonetheless, the bias for both Cologne and Berlin suggests that air temperatures are underestimated during the cooling and coldest periods.

Table 4. Evaluation metrics for the first child domain (8 m horizontal resolution) in all three cities divided into temporal clusters

	Dortmund				**Cologne**				**Berlin**			
Time group	Hot	Cold	Warming	Cooling	Hot	Cold	Warming	Cooling	Hot	Cold	Warming	Cooling
Pearson r	0.58	0.32	0.76	0.84	0.72	0.44	0.87	0.85	0.79	0.81	0.88	0.75
R^2	0.34	0.10	0.58	0.71	0.51	0.19	0.76	0.73	0.58	0.65	0.78	0.57
RMSE (°C)	1.94	1.64	2.16	1.17	1.95	2.01	1.14	2.38	1.81	2.22	1.29	1.90
IoA	0.75	0.57	0.79	0.91	0.81	0.53	0.93	0.78	0.87	0.66	0.93	0.81
Bias (°C)	0.30	-0.05	-1.43	0.30	0.67	1.59	0.32	2.04	0.18	2.01	0.02	1.14

Part of the underestimation of nighttime air temperatures can be related back to the COSMO data. The time series in Fig 3 reveals that the air temperature boundary conditions derived from the COSMO model are lower than both CROWD and PALM air temperatures for the Berlin case. A study by Radović et al. [75] highlights the importance of accurate boundary conditions. They showed that the PALM model is capable of adjusting and refining the meteorological conditions from the dynamic input, but that the boundary conditions have a strong influence on the model results. Lower air temperatures in the COSMO model can be caused by a lack of representing urban effects, especially at night. The COSMO model only considers the changed roughness of

urban areas but not their thermal properties in its land cover scheme [76, 77]. Nevertheless, the model results reveal that the PALM model is capable of "adding" an urban effect to the mesocale forcing data, resulting in higher nighttime air temperatures and highlighting the importance of explicitly modelling urban areas.

The model evaluation with CROWD data is clearly capable of detecting temporally varying model performance. The detected underestimation is acceptable considering the maximum RMSE of 2.38 °C. It can partly by related to known issues with the meteorological forcing data. To test whether the temporal patterns also exhibit a spatial component, we next examine the spatial patterns of these differences and their relationship to the urban structure.

As the spatial variability of air temperatures depends on the time of day, the aforementioned time clusters are reapplied to cover the morning and evening periods as well as the warmest and coldest periods. Spatial variability should be lower during daytime and higher during nighttime, following the concept of the UHI [2]. The PALM and CROWD air temperature for all three cities are compared within scatter plots for each time cluster (Fig 4). The plots reveal a lower spatial variability during daytime in the PALM data. After sunset, the spatial variability of the PALM data increases in all three cities, resulting in less scatter around the line of equality. For Dortmund however, the data are very scattered around the line of equality during the coldest hours, matching the low coefficient of correlation in Table 4. The low nighttime bias in Dortmund seems to result from localised overestimations and underestimations of air temperatures, which counterbalance each other when aggregated into a mean bias. The model shows an overall lower spatial variability for built areas than the CROWD data, whereas the spatial variability increases at night when spatial differences in the UHI manifest. The lower spatial variability in the PALM data is consistent between the studied cities in this paper and previous studies. The validation study in Prague [22], e.g., noted a low spatial variability in air temperature. Comparison of PALM model results with measurements from either low-cost sensors [74] or crowdsourced data [27] in Vienna also revealed lower spatial variability in the PALM data.

To further investigate the lower spatial variability of PALM nighttime air temperatures and to exclude any impact of radiation errors in the CROWD data, we averaged the air temperature differences between the PALM and CROWD data for the coldest time cluster (03:00 - 06:00 UTC) at each station and city. The resulting maps in Fig 5 reveal no distinct spatial pattern in Cologne and Berlin, with a general underestimation of nighttime air temperatures by PALM. In contrast, Dortmund shows a clear spatial pattern: air temperatures tend to be underestimated in the dense urban centre and overestimated towards the edges of the city. This suggests that the density of the urban form conceivably influences the accuracy of PALM, yet this pattern is not found in Cologne and Berlin. This is possibly due to the larger size of these cities resulting in the modelling domains covering fewer low-density areas. Focusing on the denser city centre in Dortmund (Fig 5), PALM underestimates nighttime air temperatures mirroring the findings for Cologne and Berlin. This is consistent with the evaluation study with crowdsourced air temperature data in Vienna which revealed an underestimation of nighttime air temperatures in the dense city centre and an overestimation towards the edges of the city [27]. Similarly, an intercomparison of four urban climate models for the city of Bern indicated that PALM overestimated air temperatures towards the edges of the city [78], supporting our findings for the Dortmund case.

In order to analyse the influence of the urban form on the model results, we calculated the regression of the air temperature differences between the PALM and CROWD data with the sky view factor (SVF) at the stations' location, the mean building height within a 20 m radius, the degree of imperviousness within a 200 m

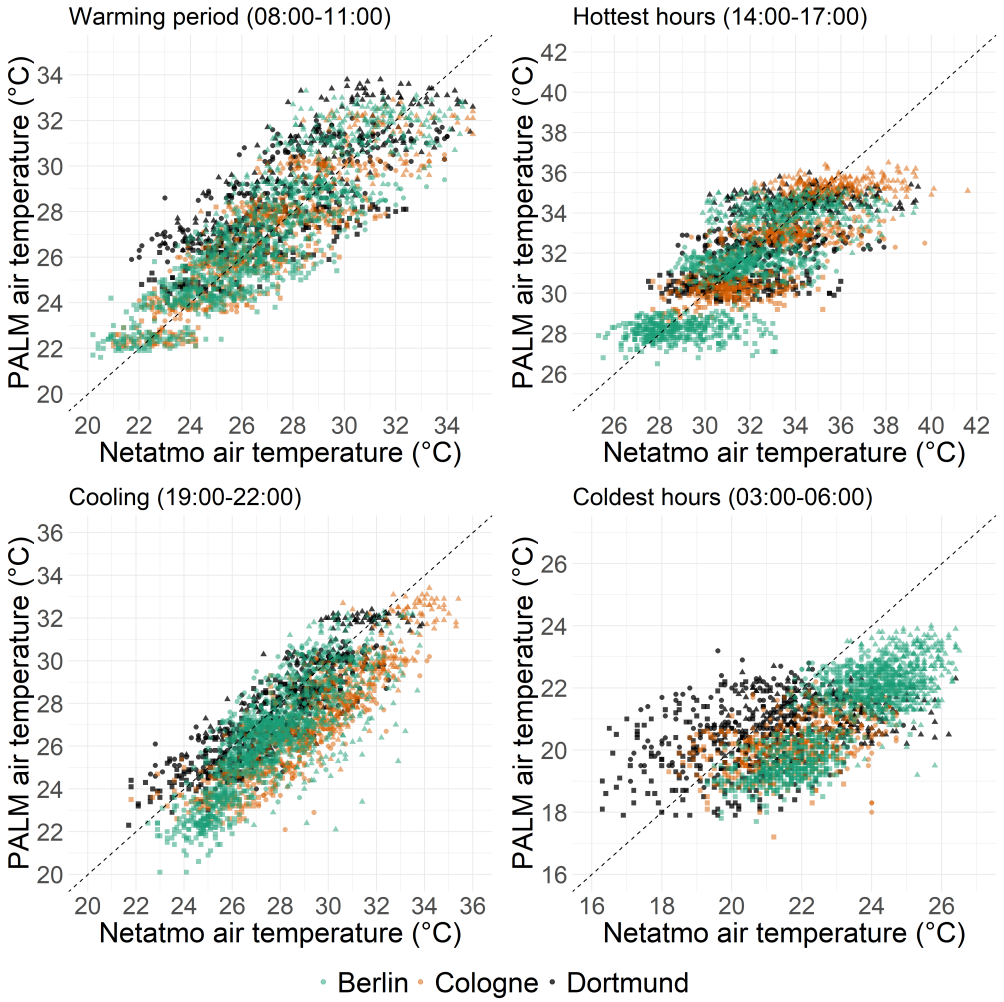

Fig 4. Scatter plots of the modelled and measured air temperature (°C) data for time cluster covering the warmest and coldest hours as well as the warming and cooling periods for all three cities. Green dots represent the data for Berlin, orange dots the data for Cologne and black dots the data for Dortmund. Each scatter plot contains the line of equality (1:1 line) to highlight the relationship between the datasets (dashed line).

radius, and the distance to green areas with a minimum size of 100 m^2. The resulting coefficient of determination time series in Fig 6 reveal no pattern for Cologne. For Dortmund and Berlin, there are weak relationships between the SVF and air temperature differences during the second (Dortmund) or first half (Berlin) of the night. This aligns well with the previous observation that the density of the urban areas influences the modelling accuracy.

In addition to the temporal patterns in model accuracy, the evaluation with CROWD data detected a spatial pattern in model accuracy. Furthermore, the observed patterns align with findings from previous studies [22, 27, 74, 78]. Next potential causes for the model errors are discussed.

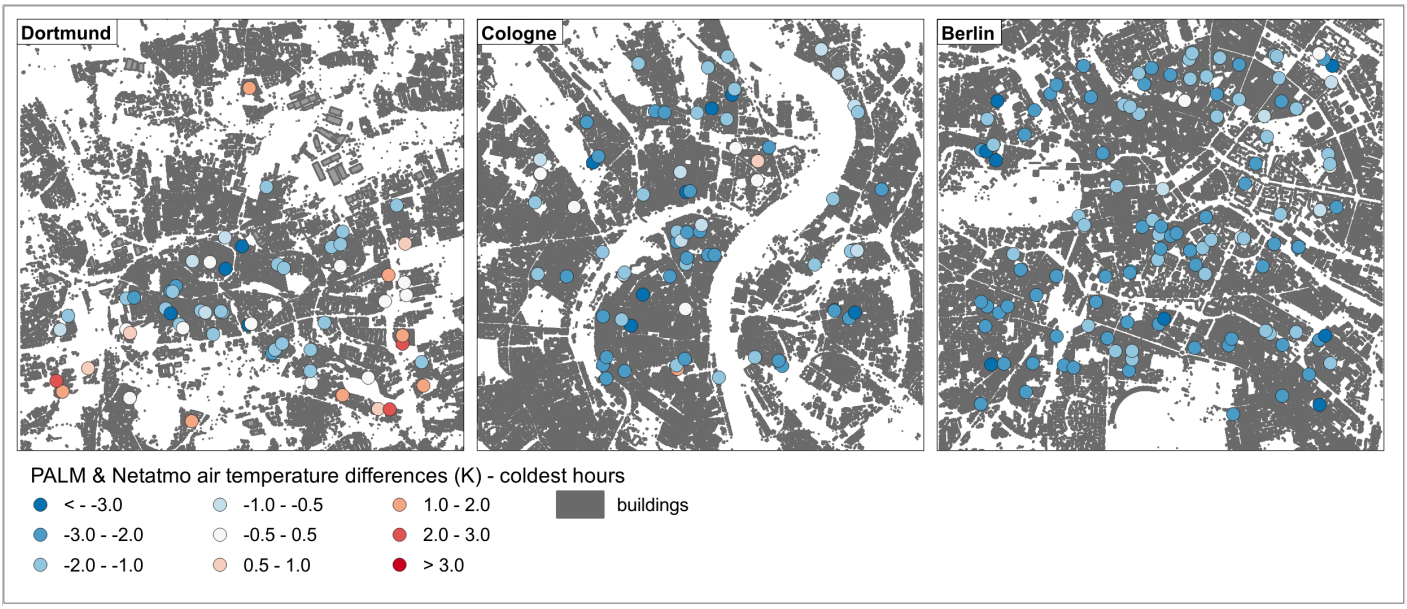

Fig 5. Mean air temperature differences (K) between the modelled and the measured data for the three coldest hours of the simulation period in Dortmund (left), Cologne (middle) and Berlin (right). Air temperature differences are averaged for each station and city during the coldest hours (03:00 - 06:00 UTC)

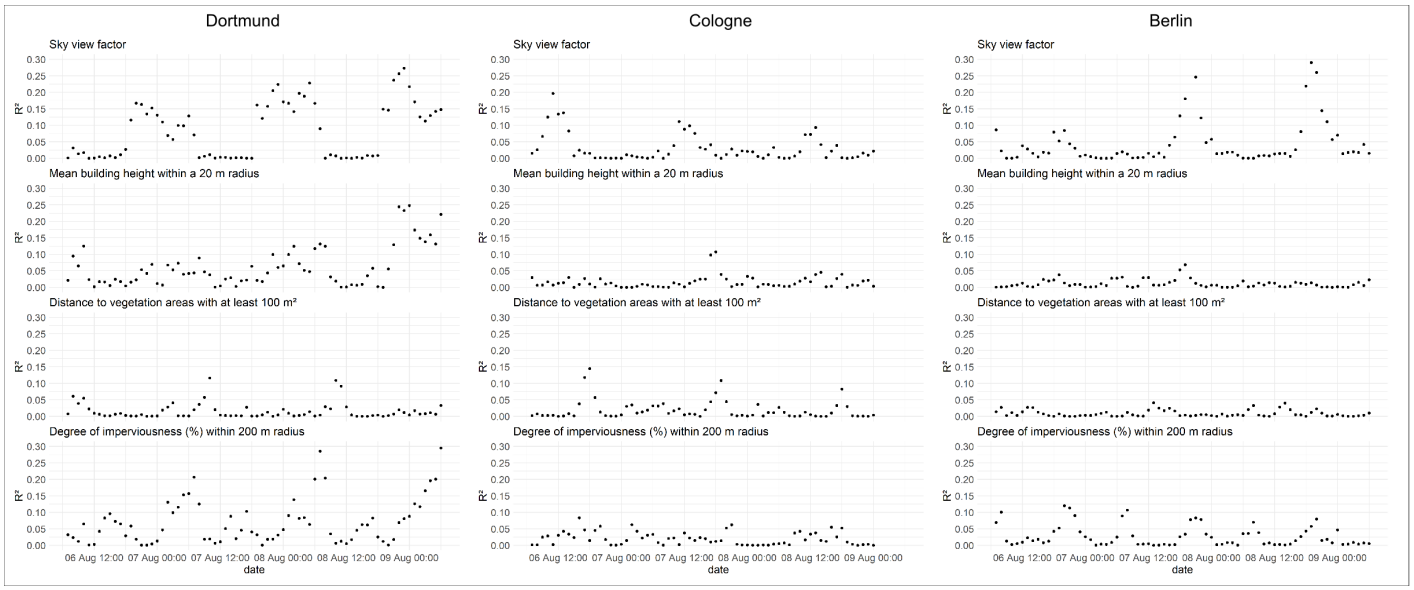

Fig 6. Time series of the regression of air temperature differences (K) between model and measurement against parameters of urban structure and vegetation in Dortmund (left), Cologne (middle) and Berlin (right). Parameters of urban structure and vegetation are: the sky view factor at the stations location (top), the mean building height within a 20 m radius (second from the top), the degree of imperviousness within a 200 m radius (third from the top) and the distance to green areas with a minimum size of 100 m² (bottom). Regressions are calculated for every parameter against the air temperature differences for every simulated hour.

Inaccuracies of the model and model input data

Model inaccuracies can originate both from within the model as well as from the provided input data. The nighttime underestimation of air temperatures can partly be

related to the COSMO forcing data as discussed above. Beyond the forcing data, LES models have known difficulties modelling (nocturnal) stable boundary layers. PALM tends to overestimate the stability of the nocturnal boundary layer in the lower levels, creating a shallower boundary layer [45, 79, 80]. For relatively coarse grid spacings down to 2 m, a revised version of PALM's subgrid-scale turbulence parametrisation led to improved grid convergence [79]. However, a follow-up study gave evidence that for smaller grid spacings, issues persist [80]. A misrepresentation of the nocturnal stable boundary layer thus can lead to various issues such as the underestimation of ventilation within urban canyons resulting in overestimated air pollutant concentrations [81] or an overestimated cooling leading to the observed underestimation of nighttime air temperatures [45].

The observed spatial patterns in model accuracy further indicate urban density influences the modelling results. As such, another potential shortcoming can be the representation of 3D radiation fluxes within the urban canopy. At night, longwave radiation processes are particularly important. The reported weak relationship between the SVF and air temperatures differences in Dortmund and Berlin in Fig 6 indicates that longwave radiation trapping is correlated with air temperature differences. High-density urban areas (low SVF) exhibit a higher underestimation of air temperatures as shown above. This suggests that some radiative processes may not be fully represented in the model.

Inaccurate input data can also introduce uncertainties into the model. Comparing the initial meteorological conditions for all three cities reveals high initial soil moisture values for Cologne. Elevated soil moisture can enhance cooling through evapotranspiration from vegetation. Belda et al. [82] demonstrated a noticeable sensitivity of the model to soil moisture in the vicinity of vegetated surfaces. However, considering the whole model domain, the effect was negligible. At the same time, the studied domain in Cologne had a high degree of sealed surfaces. Therefore, the high initial soil moisture in Cologne can only partly explain the underestimation of nighttime air temperatures.

In addition to the dynamic input data, the static input data representing the urban form and fabric are highly relevant [51]. One important aspect is the representation of trees as longwave radiation processes with the tree canopy significantly impact model results [83]. The tree data in this study are derived from 3D laser scanning data which are routinely produced in winter. Trees and crown sizes might hence be systematically underestimated. This potentially leads to lower nighttime air temperatures due to reduced heat trapping underneath the trees.

Furthermore, inaccuracies in the prescribed surface and building properties can reduce the model's ability to capture spatiotemporal variability. The thermal and radiative properties of artificial surfaces are defined by the definition of surface and building types within the static driver [51]. In practice, detailed data are often lacking and microscale variations in the surface and building properties may not be captured. Simultaneously, the emitted longwave radiation strongly depends on surface properties such as emissivity [83]. This can lead to inaccuracies in the emitted longwave radiation. As the model is sensitive to parameters such as, albedo, emissivity, thermal conductivity of walls, and volumetric heat capacity [82], improving this information in the static driver could improve the representation of spatiotemporal variations in air temperature.

Inaccuracies of the measurement data

While some differences between the PALM and CROWD data can be attributed to the PALM model, the observational data also contain inaccuracies, which become evident in this comparison. For example, time series from individual stations in Dortmund's second child domain (Fig 7) show excellent agreement between PALM and CROWD

data at certain locations, such as stations 29301, 29308, and 126350. This is reflected in the high correlation coefficients and coefficients of determination in Table 3, and is consistent with results from Cologne, Berlin (S1 Fig, S2 Fig), and a previous study in Bochum [26]. However, the comparison also reveals errors in the CROWD data. Despite rigorous quality control, radiation errors remain a prominent feature within the dataset during daytime, as can be seen in the outliers at station 126349. When Fenner et al. [30] developed the quality control procedure, they noted that the filtered dataset likely retained some radiative errors as positive deviations remained between the crowdsourced and reference data at daytime during summer. This causes a mismatch between the PALM and CROWD data, indicating a lower model performance, while the discrepancy originates from the measurements. Additionally, missing data points during the warming or cooling periods, as observed at stations 29305, 29313, and 29473, indicate faulty measurements that were removed during quality control.

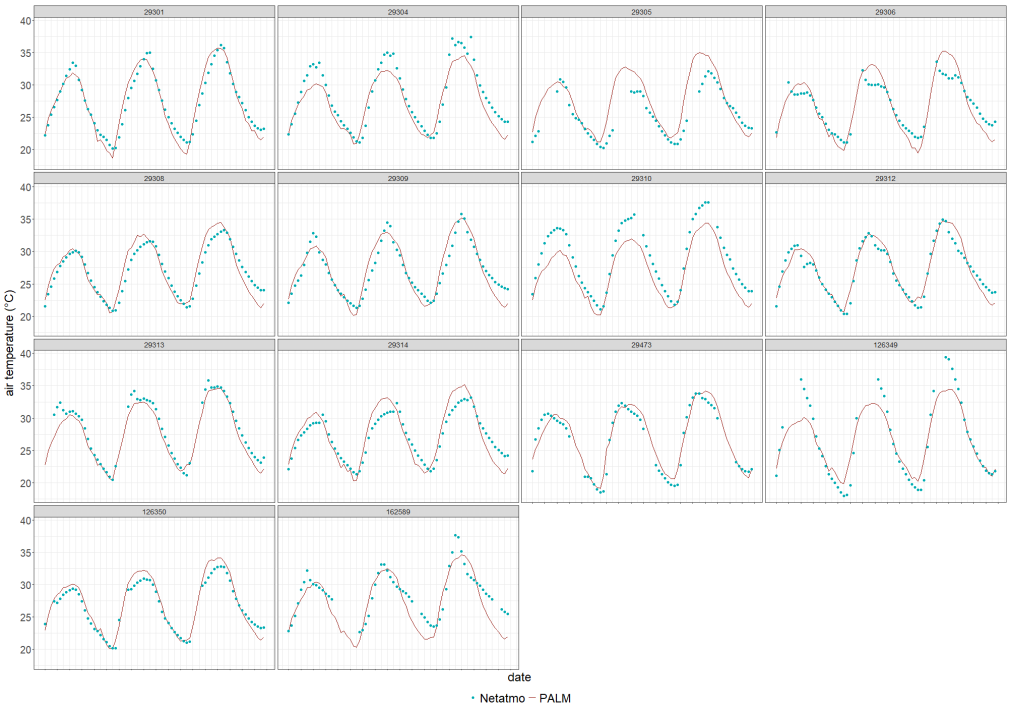

Fig 7. Time series of modelled and measured air temperature data (°C) for the finest child domain in Dortmund for each individual station position. Data displayed covers the simulated period from the 6th of August 07:00 UTC to the 9th of August 06:00 UTC.

Another limitation of the CROWD data is missing or inaccurate metadata, particularly regarding station location and installation height. Mismatches between the PALM and CROWD data can result from inaccurate location information and/or by the exclusion of the PALM air temperature above roof level. For instance, stations 29306, 29310, and 162589 show discrepancies between PALM and CROWD time series (Fig 7). Examining the location of those stations and their representation in the static driver of PALM model gives insight into potential causes for the mismatches (Fig 8). The CROWD data at stations 29306 and 162589 are either higher or lower than the PALM data at midday which suggests that these mismatches are due to differences in shading or solar exposure not captured by the model. For example, station 29306 (Fig 8 left panel) is only slightly shaded in the model but appears more shaded in the

measurements, while station 162589 (Fig 8 middle panel) is modelled as shaded but shows evidence of direct solar radiation in the observations. Therefore, the mismatches are likely not caused by inaccuracies of the model, but rather by inaccurate locations in the measurement metadata. These examples show that validation works in both directions: while measurements inform model evaluation, the model also helps identify residual errors in the observational data.

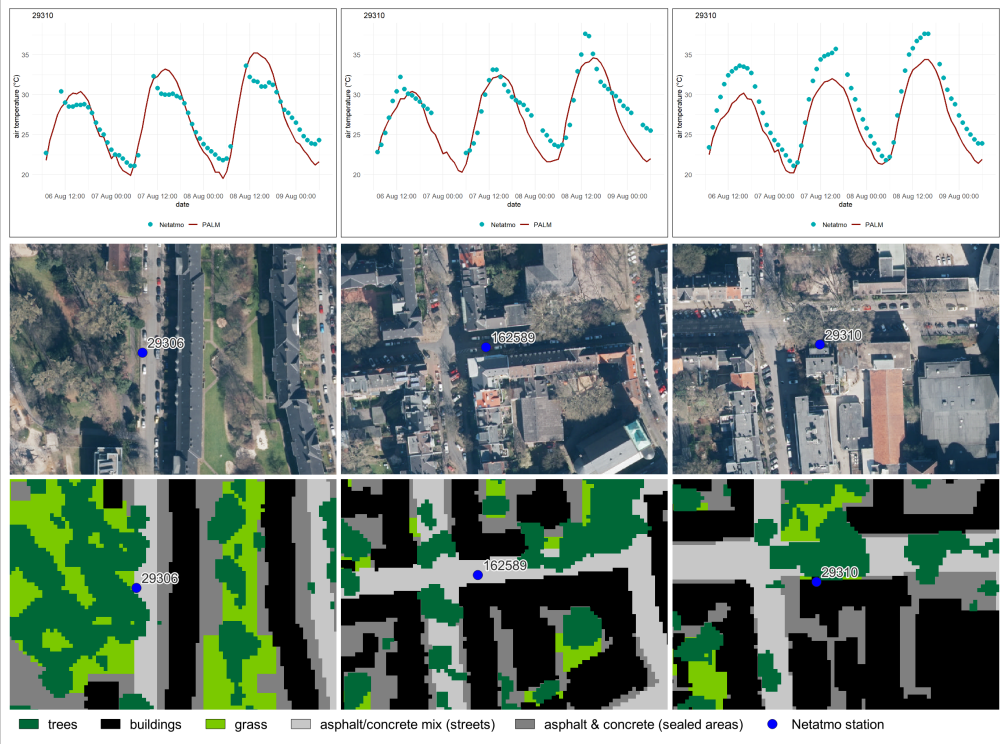

Fig 8. Differences between the model and the measurement caused by the data extraction method or inaccurate metadata of the measurements. Detection of differences through visual comparison of the time series of PALM and Netatmo at individual stations (top panels), their respective location (middle panels) and representation of the location within the static driver of the PALM model (bottom panels).

The lack of metadata on installation height further complicates comparisons, as all measurements are compared to modelled 2 m air temperatures. This leads to microscale influences on the measurements, which cannot be captured by the model directly as the exact location of each station is unknown. For example, a station on a roof terrace may be compared to modelled data representing street-level conditions beneath a tree (Fig 8, right panel), leading to lower modelled daytime temperatures.

Furthermore, placement of stations close to walls can influence the measurements significantly [29] while the specific thermal and radiative properties of the walls are not known and can only be approximated within PALM [51]. This can cause deviations between the model and the measurement, particularly in the near vicinity of walls/buildings. Such microscale influences are difficult to identify and correct, especially given the limited metadata. Consequently, due to microscale influences in the measurements [29], residual radiation errors [30] and the inaccurate metadata, data from a single station are not suitable for robust model evaluation. Instead, aggregating data from multiple stations enables the study of urban heat island (UHI) effects and

spatial temperature variations [25, 28, 32] and model evaluation as demonstrated here and in previous studies [26, 27]. However, this approach is limited to modelling domains with a sufficient number of stations and only allows for the evaluation of the model results in the proximity of buildings as CWS are installed where people live. Green spaces like parks, forests or fields are not represented by the measurements [31].

Conclusion

This study investigated the use of crowdsourced air temperature data for the evaluation of PALM model simulations. Previous studies [26, 27] already indicated a considerable potential but were limited to a single city. The current studied applied the model evaluation to three cities with different geographical characteristics. Based on our results, the research questions can be answered:

To what extent does the microscale LES model PALM improve the representation of the urban thermal effect in relation to the mesoscale forcing data?

Even though the PALM model underestimated nighttime air temperatures, the model results for Berlin clearly show that PALM can effectively correct for the missing urban effect within the COSMO forcing data, which led to low air temperatures in the PALM data. This furthermore highlights the importance of explicitly modelling of urban areas. The nighttime underestimation of air temperatures in Dortmund and Cologne, however, are not caused by low air temperatures in the forcing data.

Are there any temporal and / or spatial patterns in the differences between the modelled and crowdsourced data and what causes the spatiotemporal patterns? Can differences be attributed to errors in either the model or the crowdsourced data?

Both Cologne and Berlin exhibit a general underestimation of nighttime air temperatures in the model, whereas this underestimation is limited to the dense city centre in Dortmund. All three cities reveal lower spatial air temperature variability in the model than in the measurements consistent with previous studies [27, 74].

A part of the underestimation of nighttime air temperatures can be attributed to low air temperatures in the boundary conditions. Furthermore, as an LES model, PALM has known issues modelling the stable (nocturnal) boundary layer. The detected spatial patterns suggest a misrepresentation of radiative processes within the urban canopy. While some possible reasons for the underestimation were tested and discussed, a final attribution was not possible.

On the observational side, inaccurate metadata and residual radiation errors within the crowdsourced data caused mismatches between both datasets for some stations.

What are the benefits and limitations of model evaluation with crowdsourced air temperature data? Is the model evaluation with crowdsourced data consistent between different cities?

The high spatial and temporal coverage of the crowdsourced air temperature data proved valuable for the evaluation of intra-urban air temperature variability. Challenges arise from inaccurate metadata of the crowdsourced data and inherent radiation errors after quality control. This limits the evaluation with crowdsourced data to model domains with a sufficient number of CWS to generate reliable information. The evaluation with this type of crowdsourced data is limited to the vicinity of buildings and the models performance in modelling the thermal conditions within green spaces cannot be evaluated. The evaluation of the model results with crowdsourced data was applied in three cities with different sizes and geographical settings. In all cities, the evaluation revealed a good model performance with a well represented diurnal cycle. At the same time, nighttime underestimations of air temperatures were observed in all three cities.

Future studies using both crowdsourced and high-accuracy observational data might focus on determining the causes of the nighttime underestimation by performing

sensitivity studies. More parameters besides air temperature may be incorporated, as thermal exposure does not only depend on the air temperature [12, 13]. Sensitivity tests should also consider boundary conditions from a different mesoscale model such as ICON or WRF, different turbulence closure methods to represent stable conditions, changes in surface properties and improved tree representation to determine the influence of the level of detail of the static input data.

The modelled air temperature data can identify weaknesses in the measured data, including radiation errors or inaccurate metadata. Future studies could explore the potential of refining the quality control procedure of crowdsourced data with the help of model output data.

The evaluation of the microscale model PALM with crowdsourced air temperature data has the potential to be a powerful tool in urban climate adaptation as it yields high resolution information on the urban microclimate and the overall validity can be proved with crowdsourced data. This approach is independent of measurement campaigns and dense professional measurement networks. Both the PALM model as well as the crowdsourced data are openly accessible making this combination fair and applicable to a variety of modelling objectives and study areas.

Supporting information

S1 Fig. Time series of modelled and measured air temperature data [°C] for the finest child domain in Cologne for each individual station position. Data displayed covers the simulated period from the 6th of August 07:00 UTC to the 9th of August 00:00 UTC.

S2 Fig. Time series of modelled and measured air temperature data [°C] for the finest child domain in Berlin for each individual station position. Data displayed covers the simulated period from the 6th of August 07:00 UTC to the 9th of August 06:00 UTC.

S1 Table. Information on the geodatasets used as a basis to generate the required information for the static driver.

S2 Table. Evaluation metrics for the second child domain (2 m horizontal resolution) in all three cities

Acknowledgments

B.M. was partly funded with resources from zukunft.niedersachsen, a funding program of the Lower Saxony Ministry of Science and Culture and VolkswagenStiftung. The authors gratefully acknowledge the computing time made available to them on the high-performance computer "Lise" at the NHR center NHR@ZIB. This center is jointly supported by the Federal Ministry of Education and Research and the state governments participating in the NHR (www.nhr-verein.de).

References

1. United Nations, Department of Economic and Social Affairs, Population Division. World UrbanizationProspects: The 2018 Revision (ST/ESA/SER.A/420); 2019. Available from: `https://population.un.org/wup/Publications/`.

2. Oke TR, Mills G, Christen A, Voogt JA. Urban Climates. Cambridge: Cambridge University Press; 2017. Available from: http://ebooks.cambridge.org/ref/id/CBO9781139016476.

3. García-León D, Casanueva A, Standardi G, Burgstall A, Flouris AD, Nybo L. Current and projected regional economic impacts of heatwaves in Europe. Nature Communications. 2021;12(1):5807. doi:10.1038/s41467-021-26050-z.

4. Szewczyk W, Mongelli I, Ciscar JC. Heat stress, labour productivity and adaptation in Europe—a regional and occupational analysis. Environmental Research Letters. 2021;16(10):105002. doi:10.1088/1748-9326/ac24cf.

5. De Sario M, de'Donato FK, Bonafede M, Marinaccio A, Levi M, Ariani F, et al. Occupational heat stress, heat-related effects and the related social and economic loss: a scoping literature review. Frontiers in Public Health. 2023;11. doi:10.3389/fpubh.2023.1173553.

6. Kovats RS, Hajat S. Heat Stress and Public Health: A Critical Review. Annual Review of Public Health. 2008;29(Volume 29, 2008):41–55. doi:10.1146/annurev.publhealth.29.020907.090843.

7. Ballester J, Quijal-Zamorano M, Méndez Turrubiates RF, Pegenaute F, Herrmann FR, Robine JM, et al. Heat-related mortality in Europe during the summer of 2022. Nature Medicine. 2023;29(7):1857–1866. doi:10.1038/s41591-023-02419-z.

8. Robine JM, Cheung SLK, Roy SL, Oyen HV, Griffiths C, Michel JP, et al. Death toll exceeded 70,000 in Europe during the summer of 2003. Comptes Rendus Biologies. 2008;331(2):171–178. doi:10.1016/j.crvi.2007.12.001.

9. Heaviside C, Vardoulakis S, Cai XM. Attribution of mortality to the urban heat island during heatwaves in the West Midlands, UK. Environmental Health. 2016;15(1):S27. doi:10.1186/s12940-016-0100-9.

10. Intergovernmental Panel on Climate Change (IPCC). Climate Change 2021 – The Physical Science Basis: Working Group I Contribution to the Sixth Assessment Report of the Intergovernmental Panel on Climate Change. Cambridge: Cambridge University Press; 2023. Available from: https://www.cambridge.org/core/books/climate-change-2021-the-physical-science-basis/415F29233B8BD19FB55F65E3DC67272B.

11. Heaviside C, Macintyre H, Vardoulakis S. The Urban Heat Island: Implications for Health in a Changing Environment. Current Environmental Health Reports. 2017;4(3):296–305. doi:10.1007/s40572-017-0150-3.

12. Geletič J, Lehnert M, Resler J, Krč P, Bureš M, Urban A, et al. Heat exposure variations and mitigation in a densely populated neighborhood during a hot day: Towards a people-oriented approach to urban climate management. Building and Environment. 2023;242:110564. doi:10.1016/j.buildenv.2023.110564.

13. Geletič J, Lehnert M, Krč P, Resler J, Krayenhoff ES. High-Resolution Modelling of Thermal Exposure during a Hot Spell: A Case Study Using PALM-4U in Prague, Czech Republic. Atmosphere. 2021;12(2):175. doi:10.3390/atmos12020175.

14. Toparlar Y, Blocken B, Maiheu B, van Heijst GJF. A review on the CFD analysis of urban microclimate. Renewable and Sustainable Energy Reviews. 2017;80:1613–1640. doi:10.1016/j.rser.2017.05.248.

15. Bruse M, Fleer H. Simulating surface–plant–air interactions inside urban environments with a three dimensional numerical model. Environmental Modelling & Software. 1998;13(3):373–384. doi:10.1016/S1364-8152(98)00042-5.

16. Suter I, Grylls T, Sützl BS, Owens SO, Wilson CE, van Reeuwijk M. uDALES 1.0: a large-eddy simulation model for urban environments. Geoscientific Model Development. 2022;15(13):5309–5335. doi:10.5194/gmd-15-5309-2022.

17. Maronga B, Banzhaf S, Burmeister C, Esch T, Forkel R, Fröhlich D, et al. Overview of the PALM model system 6.0. Geoscientific Model Development. 2020;13(3):1335–1372. doi:10.5194/gmd-13-1335-2020.

18. Geletič J, Lehnert M, Resler J, Krč P, Middel A, Krayenhoff ES, et al. High-fidelity simulation of the effects of street trees, green roofs and green walls on the distribution of thermal exposure in Prague-Dejvice. Building and Environment. 2022;223:109484. doi:10.1016/j.buildenv.2022.109484.

19. Heris MP, Middel A, Muller B. Impacts of form and design policies on urban microclimate: Assessment of zoning and design guideline choices in urban redevelopment projects. Landscape and Urban Planning. 2020;202:103870. doi:10.1016/j.landurbplan.2020.103870.

20. Anders J, Schubert S, Sauter T, Tunn S, Schneider C, Salim M. Modelling the impact of an urban development project on microclimate and outdoor thermal comfort in a mid-latitude city. Energy and Buildings. 2023;296:113324. doi:10.1016/j.enbuild.2023.113324.

21. Gronemeier T, Surm K, Harms F, Leitl B, Maronga B, Raasch S. Evaluation of the dynamic core of the PALM model system 6.0 in a neutrally stratified urban environment: comparison between LES and wind-tunnel experiments. Geoscientific Model Development. 2021;14(6):3317–3333. doi:10.5194/gmd-14-3317-2021.

22. Resler J, Eben K, Geletič J, Krč P, Rosecký M, Sühring M, et al. Validation of the PALM model system 6.0 in a real urban environment: a case study in Dejvice, Prague, the Czech Republic. Geoscientific Model Development. 2021;14(8):4797–4842. doi:10.5194/gmd-14-4797-2021.

23. Harlan SL, Brazel AJ, Prashad L, Stefanov WL, Larsen L. Neighborhood microclimates and vulnerability to heat stress. Social science & medicine (1982). 2006;63(11):2847–2863. doi:10.1016/j.socscimed.2006.07.030.

24. Muller CL, Chapman L, Johnston S, Kidd C, Illingworth S, Foody G, et al. Crowdsourcing for climate and atmospheric sciences: current status and future potential. International Journal of Climatology. 2015;35(11):3185–3203. doi:10.1002/joc.4210.

25. Vulova S, Meier F, Fenner D, Nouri H, Kleinschmit B. Summer Nights in Berlin, Germany: Modeling Air Temperature Spatially With Remote Sensing, Crowdsourced Weather Data, and Machine Learning. IEEE Journal of Selected Topics in Applied Earth Observations and Remote Sensing. 2020;13:5074–5087. doi:10.1109/JSTARS.2020.3019696.

26. van der Linden L, Hogan P, Maronga B, Hagemann R, Bechtel B. Crowdsourcing air temperature data for the evaluation of the urban microscale model PALM—A case study in central Europe. PLOS Climate. 2023;2(8):e0000197. doi:10.1371/journal.pclm.0000197.

27. Žuvela Aloise M, Hahn C, Hollósi B. Evaluation of city-scale PALM model simulations and intra-urban thermal variability in Vienna, Austria using operational and crowdsourced data. Urban Climate. 2025;59:102245. doi:10.1016/j.uclim.2024.102245.

28. Meier F, Fenner D, Grassmann T, Otto M, Scherer D. Crowdsourcing air temperature from citizen weather stations for urban climate research. Urban Climate. 2017;19:170–191. doi:10.1016/j.uclim.2017.01.006.

29. Napoly A, Grassmann T, Meier F, Fenner D. Development and Application of a Statistically-Based Quality Control for Crowdsourced Air Temperature Data. Frontiers in Earth Science. 2018;6:118. doi:10.3389/feart.2018.00118.

30. Fenner D, Bechtel B, Demuzere M, Kittner J, Meier F. CrowdQC+—A Quality-Control for Crowdsourced Air-Temperature Observations Enabling World-Wide Urban Climate Applications. Frontiers in Environmental Science. 2021;9. doi:10.3389/fenvs.2021.720747.

31. Fenner D, Meier F, Bechtel B, Otto M, Scherer D. Intra and inter 'local climate zone' variability of air temperature as observed by crowdsourced citizen weather stations in Berlin, Germany. Meteorologische Zeitschrift. 2017;26(5):525–547. doi:10.1127/metz/2017/0861.

32. Kittner J, Fenner D, Demuzere M, Bechtel B. Analysis of nocturnal urban heat advection using crowd weather stations. Quarterly Journal of the Royal Meteorological Society;n/a(n/a):e5065. doi:10.1002/qj.5065.

33. Bundesamt S. Städte (Alle Gemeinden mit Stadtrecht) nach Fläche, Bevölkerung und Bevölkerungsdichte am 31.12.2023;. Available from: `https://www.destatis.de/DE/Themen/Laender-Regionen/Regionales/Gemeindeverzeichnis/Administrativ/05-staedte.html`.

34. Bissolli P, Dittmann E. The objective weather type classification of the German Weather Service and its possibilities of application to environmental and meteorological investigations. Meteorologische Zeitschrift. 2001; p. 253–260. doi:10.1127/0941-2948/2001/0010-0253.

35. (DWD) DW. Objective Weather Type Classification Data; 2025. Available from: `https://www.dwd.de/EN/ourservices/wetterlagenklassifikation/online_wlkdaten.txt?view=nasPublication&nn=495490`.

36. (CDC) DCDC. 10-minute values of station observations of air temperature 2 m above ground in °C for Germany, version v21.3; 2025.

37. (CDC) DCDC. Hourly mean of station observations of wind speed ca. 10 m above ground in m/s for Germany, version v21.3; 2025.

38. (CDC) DCDC. Hourly station observations of relative humidity in % for Germany, version v21.3; 2025.

39. (CDC) DCDC. Hourly station observations of cloud coverage in eighths for Germany, version v21.3; 2025.

40. Deardorff JW. Stratocumulus-capped mixed layers derived from a three-dimensional model. Boundary-Layer Meteorology. 1980;18(4):495–527. doi:10.1007/BF00119502.

41. Moeng CH, Wyngaard JC. Spectral Analysis of Large-Eddy Simulations of the Convective Boundary Layer. Journal of the Atmospheric Sciences. 1988;45(23):3573–3587. doi:10.1175/1520-0469(1988)045

42. Saiki EM, Moeng CH, Sullivan PP. Large-Eddy Simulation Of The Stably Stratified Planetary Boundary Layer. Boundary-Layer Meteorology. 2000;95(1):1–30. doi:10.1023/A:1002428223156.

43. Wicker LJ, Skamarock WC. Time-Splitting Methods for Elastic Models Using Forward Time Schemes. Monthly Weather Review. 2002;130(8):2088–2097. doi:10.1175/1520-0493(2002)130¡2088:TSMFEM¿2.0.CO;2.

44. Maronga B, Gryschka M, Heinze R, Hoffmann F, Kanani-Sühring F, Keck M, et al. The Parallelized Large-Eddy Simulation Model (PALM) version 4.0 for atmospheric and oceanic flows: model formulation, recent developments, and future perspectives. Geoscientific Model Development. 2015;8(8):2515–2551. doi:10.5194/gmd-8-2515-2015.

45. Gehrke KF, Sühring M, Maronga B. Modeling of land–surface interactions in the PALM model system 6.0: land surface model description, first evaluation, and sensitivity to model parameters. Geoscientific Model Development. 2021;14(8):5307–5329. doi:10.5194/gmd-14-5307-2021.

46. Resler J, Krč P, Belda M, Juruš P, Benešová N, Lopata J, et al. PALM-USM v1.0: A new urban surface model integrated into the PALM large-eddy simulation model. Geoscientific Model Development. 2017;10(10):3635–3659. doi:10.5194/gmd-10-3635-2017.

47. Krč P, Resler J, Sühring M, Schubert S, Salim MH, Fuka V. Radiative Transfer Model 3.0 integrated into the PALM model system 6.0. Geoscientific Model Development. 2021;14(5):3095–3120. doi:10.5194/gmd-14-3095-2021.

48. Fröhlich D, Matzarakis A. Calculating human thermal comfort and thermal stress in the PALM model system 6.0. Geoscientific Model Development. 2020;13(7):3055–3065. doi:10.5194/gmd-13-3055-2020.

49. Kadasch E, Sühring M, Gronemeier T, Raasch S. Mesoscale nesting interface of the PALM model system 6.0. Geoscientific Model Development. 2021;14(9):5435–5465. doi:10.5194/gmd-14-5435-2021.

50. Hellsten A, Ketelsen K, Sühring M, Auvinen M, Maronga B, Knigge C, et al. A nested multi-scale system implemented in the large-eddy simulation model PALM model system 6.0. Geoscientific Model Development. 2021;14(6):3185–3214. doi:10.5194/gmd-14-3185-2021.

51. Heldens W, Burmeister C, Kanani-Sühring F, Maronga B, Pavlik D, Sühring M, et al. Geospatial input data for the PALM model system 6.0: model requirements, data sources and processing. Geoscientific Model Development. 2020;13(11):5833–5873. doi:10.5194/gmd-13-5833-2020.

52. European Environment Agency. CORINE Land Cover 2018 (vector), Europe, 6-yearly - version 2020_20u1, May 2020; 2019. Available from: `https://sdi.eea.europa.eu/catalogue/copernicus/api/records/71c95a07-e296-44fc-b22b-415f42acfdf0?language=all`.

53. Geologischer Dienst NRW. IS BK 50 Bodenkarte von NRW 1 : 50.000: licence: dl-de/by-2-0; 2023. Available from: `https://www.bezreg-koeln.nrw.de/geobasis-nrw/produkte-und-dienste/hoehenmodelle/3d-messdaten`.

54. Senatsverwaltung für Stadtentwicklung, Bauen und Wohnen Berlin. Boden im INSPIRE-Datenmodell (Bodengesellschaften und Bodenarten 2020); 2024. Available from: https://gdi.berlin.de/geonetwork/srv/ger/catalog.search#/metadata/0b5846bb-1f00-3f12-866e-d9dd29380379.

55. Bundesamt für Kartographie und Geodäsie. Digitales Geländemodell Gitterweite 200 m (DGM200): licence: dl-de/by-2-0; 2023. Available from: https://gdz.bkg.bund.de/index.php/default/digitale-geodaten/digitale-gelandemodelle/digitales-gelandemodell-gitterweite-200-m-dgm200.html.

56. NRW G. ALKIS Grundrissdaten; 2024. Available from: https://www.bezreg-koeln.nrw.de/geobasis-nrw/produkte-und-dienste/liegenschaftskataster/aktuelles-liegenschaftskataster.

57. Senatsverwaltung für Stadtentwicklung, Bauen und Wohnen Berlin. ALKIS Berlin; 2024. Available from: https://gdi.berlin.de/geonetwork/srv/ger/catalog.search#/metadata/0a7c53a5-b29d-3f45-9734-1c811045e6c2.

58. European Environment Agency. Imperviousness Density 2018 (raster 10 m), Europe, 3-yearly, Aug. 2020; 2020. Available from: https://sdi.eea.europa.eu/catalogue/copernicus/api/records/3bf542bd-eebd-4d73-b53c-a0243f2ed862?language=all.

59. Geobasis NRW. 3D-Gebäudemodell LoD2 (CityGML): licence: dl-de/by-2-0; 2024. Available from: https://www.bezreg-koeln.nrw.de/geobasis-nrw/produkte-und-dienste/3d-gebaeudemodelle.

60. Senatsverwaltung für Stadtentwicklung, Bauen und Wohnen Berlin. 3D-Gebäudemodelle im Level of Detail 2 (LoD 2); 2024. Available from: https://gdi.berlin.de/geonetwork/srv/ger/catalog.search#/metadata/3c7c49af-00a4-3bcd-bc00-20e7f0f1b7bf.

61. Ämter des Bundes und der Länder S. Zensus 2011: Wohnungen und Gebäude je Hektar; 2018.

62. BKG GD. Geographische Gitter für Deutschland in UTM-Projektion 100 m; 2023. Available from: https://gdz.bkg.bund.de/index.php/default/geographische-gitter-fur-deutschland-in-utm-projektion-geogitter-national html?___SID=S.

63. Geobasis NRW. Digitales Geländemodell - Gitterweite 1m (XYZ & TIFF): licence: dl-de/by-2-0; 2024. Available from: https://www.bezreg-koeln.nrw.de/geobasis-nrw/produkte-und-dienste/hoehenmodelle/digitale-gelaendemodelle/digitales-gelaendemodell.

64. Senatsverwaltung für Stadtentwicklung, Bauen und Wohnen Berlin. ATKIS® DGM (1m-Rasterweite); 2024. Available from: https://gdi.berlin.de/geonetwork/srv/ger/catalog.search#/metadata/fa02f9e1-a0df-3be1-b0aa-bc624c0c7ff5.

65. Geobasis NRW. 3D-Messdaten Laserscanning (LAS): licence: dl-de/by-2-0; 2024. Available from: https://www.bezreg-koeln.nrw.de/geobasis-nrw/produkte-und-dienste/hoehenmodelle/3d-messdaten.

66. Senatsverwaltung für Stadtentwicklung, Bauen und Wohnen Berlin. Airborne Laserscanning (ALS) Primäre 3D Laserscan-Daten; 2024. Available from: https://gdi.berlin.de/geonetwork/srv/ger/catalog.search#/metadata/f4a8997d-4dea-382f-aa3a-d452f4bf3943.

67. Geobasis NRW. Digitales Oberflächenmodell - Gitterweite 1m (TIFF): licence: dl-de/by-2-0; 2024. Available from: https://www.bezreg-koeln.nrw.de/geobasis-nrw/produkte-und-dienste/hoehenmodelle/digitale-oberflaechenmodelle/digitales.

68. Senatsverwaltung für Stadtentwicklung, Bauen und Wohnen Berlin. DOM - Digitales Oberflächenmodell; 2024. Available from: https://gdi.berlin.de/geonetwork/srv/ger/catalog.search#/metadata/5f84f650-715a-3d83-86b0-1b99fcdab360.

69. Lin D, Zhang J, Khan B, Katurji M, Revell LE. GEO4PALM v1.1: an open-source geospatial data processing toolkit for the PALM model system. Geoscientific Model Development. 2024;17(2):815–845. doi:10.5194/gmd-17-815-2024.

70. European Comission GBB Eurostat (ESTAT). Nomenclature of Territorial Units for Statistics (NUTS) - Statistical Units; 2025. Available from: https://ec.europa.eu/eurostat/web/gisco/geodata/statistical-units/territorial-units-statistics.

71. Deutscher Wetterdienst. COSMO-D2 analysis data; 2021.

72. (CDC) DCDC. Monthly grids of soil moisture under grass and sandy loam for Germany, version v19.3; 2024.

73. Kittner J, Fenner D, Demuzere M, Bechtel B. Crowd-Database — Data Description; 2025. Available from: https://ruhr-uni-bochum.sciebo.de/s/G7FdLFA6NzkPsQG?

74. Hollósi B, Žuvela Aloise M, Neureiter A, Frießenbichler M, Auferbauer P, Feigl J, et al. Capability of the building-resolving PALM model system to capture micrometeorological characteristics of an urban environment in Vienna, Austria. City and Environment Interactions. 2024;23:100152. doi:10.1016/j.cacint.2024.100152.

75. Radović J, Belda M, Resler J, Eben K, Bureš M, Geletič J, et al. Challenges of constructing and selecting the "perfect" boundary conditions for the large-eddy simulation model PALM. Geoscientific Model Development. 2024;17(7):2901–2927. doi:10.5194/gmd-17-2901-2024.

76. Trusilova K, Schubert S, Wouters H, Früh B, Grossman-Clarke S, Demuzere M, et al. The urban land use in the COSMO-CLM model: a comparison of three parameterizations for Berlin. Meteorologische Zeitschrift. 2016; p. 231–244. doi:10.1127/metz/2015/0587.

77. Doms G, Forstner J, Heise E, Reinhardt T, Ritter B, Schrodin R. A Description of the Nonhydrostatic Regional COSMO Model;. Available from: https://www.cosmo-model.org/content/model/cosmo/coreDocumentation/cosmo_physics_4.20.pdf.

78. Burger M, Gubler M, Holtmann A, Brönnimann S. Spoilt for choice - Intercomparison of four different urban climate models. Urban Climate. 2024;58:102166. doi:10.1016/j.uclim.2024.102166.

79. Dai Y, Basu S, Maronga B, de Roode SR. Addressing the Grid-Size Sensitivity Issue in Large-Eddy Simulations of Stable Boundary Layers. Boundary-Layer Meteorology. 2021;178(1):63–89. doi:10.1007/s10546-020-00558-1.

80. Maronga B, Li D. An Investigation of the Grid Sensitivity in Large-Eddy Simulations of the Stable Boundary Layer. Boundary-Layer Meteorology. 2022;182(2):251–273. doi:10.1007/s10546-021-00656-8.

81. Resler J, Bauerová P, Belda M, Bureš M, Eben K, Fuka V, et al. Challenges of high-fidelity air quality modeling in urban environments – PALM sensitivity study during stable conditions. Geoscientific Model Development. 2024;17(20):7513–7537. doi:10.5194/gmd-17-7513-2024.

82. Belda M, Resler J, Geletič J, Krč P, Maronga B, Sühring M, et al. Sensitivity analysis of the PALM model system 6.0 in the urban environment. Geoscientific Model Development. 2021;14(7):4443–4464. doi:10.5194/gmd-14-4443-2021.

83. Salim MH, Schubert S, Resler J, Krč P, Maronga B, Kanani-Sühring F, et al. Importance of radiative transfer processes in urban climate models: a study based on the PALM 6.0 model system. Geoscientific Model Development. 2022;15(1):145–171. doi:10.5194/gmd-15-145-2022.